

RICH detectors development for hadron identification at EIC: design, prototyping and reconstruction algorithm

To cite this article: L. Barion *et al* 2020 *JINST* **15** C02040

View the [article online](#) for updates and enhancements.



IOP | ebooksTM

Bringing together innovative digital publishing with leading authors from the global scientific community.

Start exploring the collection—download the first chapter of every title for free.

INTERNATIONAL WORKSHOP ON FAST CHERENKOV DETECTORS
PHOTON DETECTION, DIRC DESIGN AND DAQ
SEPTEMBER 11–13, 2019, GIESSEN, GERMANY

RICH detectors development for hadron identification at EIC: design, prototyping and reconstruction algorithm

L. Barion,^a E. Cisbani,^{b,c,1} M. Contalbrigo,^a A. Del Dotto,^d C. Fanelli,^{e,f} X. He,^g
H. van Hecke,^h Y. Ilieva,ⁱ P. Nadel-Turonski,^j X. Sun,^g C-P. Wong^g and Z.W. Zhao^k
on behalf of the EIC-eRD14 Collaboration

^aINFN Sezione di Ferrara, 44100 Ferrara, Italy

^bINFN Sezione di Roma, 00185 Rome, Italy

^cIstituto Superiore di Sanità, 00161 Rome, Italy

^dINFN Laboratori Nazionali di Frascati, 00044 Frascati (Rome), Italy

^eThomas Jefferson National Accelerator Facility, Newport News, VA 23606, U.S.A.

^fLaboratory for Nuclear Science, Massachusetts Institute of Technology, Cambridge, MA 02139, U.S.A.

^gGeorgia State University, Atlanta, GA 30303, U.S.A.

^hLos Alamos National Lab, Los Alamos, NM 87545, U.S.A.

ⁱUniversity of South Carolina, Columbia, SC 29208, U.S.A.

^jStony Brook University, Stony Brook, NY 11794, U.S.A.

^kDuke University, Durham, NC 27708, U.S.A.

E-mail: evaristo.cisbani@roma1.infn.it

ABSTRACT: The extended experimental physics program accessible with the proposed Electron-Ion Collider (EIC) strongly demands for excellent particle identification (PID) of the final state hadrons. In this context two Ring Imaging Cherenkov (RICH) detectors are under development within the EIC PID consortium (EIC-eRD14 Collaboration) explicitly formed to investigate and develop PID detectors for EIC. We present the current status of development of the two RICHes: a modular RICH detector which consists of an aerogel radiator, a Fresnel lens, a mirrored box, and pixelated photon sensor; a dual-radiator RICH, consisting of an aerogel radiator and C₂F₆ gas in a mirror-focused configuration.

KEYWORDS: Cherenkov and transition radiation; Particle identification methods

¹Corresponding author.

Contents

1	Introduction	1
2	Modular RICH	2
3	Dual-radiator RICH	3
3.1	Event-based reconstruction algorithm	6
4	Conclusions	8

1 Introduction

The detailed and extended studies of the spin and flavor structure of nucleons and nuclei and the investigation of the quantum chromodynamics at extreme parton densities, are among the main scientific goals of the ongoing Electron-Ion Collider (EIC) initiative [1].

The ambitious program of EIC is based on the measurement of inclusive, semi-inclusive and exclusive reactions of a polarized lepton (e^- and e^+) beam colliding on either a polarized p, d, ^3He or unpolarized heavier ion beam at relatively high luminosity (up to about $10^{34}/(\text{cm}^2 \cdot \text{s})$ with center of mass energy in the $\approx 20\text{--}100$ GeV range.

Two accelerator options, eRICH [2] and MLEIC [3], and, respective, similar hermetic ($\approx 4\pi$) spectrometers have been conceptually defined. Vertex and momentum resolutions down to 0.1 mm and 1% respectively, and excellent particle identifications (for hadrons and leptons) are essential common requirements for any of the EIC proposed spectrometers [4] (with solenoidal magnetic field), that share the typical segmentation of a collider spectrometers with electron and hadron endcaps and a large central barrel (see left drawing of figure 1); far-forward electrons and hadrons sectors close the spectrometer acceptance near the ion and electron beams respectively.

This paper focuses on the current development of two Ring Imaging Cherenkov (RICH) detectors [5] within the EIC-eRD14 PID consortium: the modular and the dual-radiator RICHes (mRICH and dRICH respectively) for the direct charged hadron identification in the electron and hadron endcaps at medium and high momenta.¹

The representative particles phase space for Semi-Inclusive Deep Inelastic Scattering processes is represented in the right plot of figure 1: the hadron identification shall extend to 10 GeV/c and about 50 GeV/c in the electron and hadron endcaps. Any detector in these sectors shall take into account the solenoidal magnetic field of the spectrometer and a significant level of radiation.

¹The lower momentum range ($\lesssim 3$ GeV/c) in both endcaps will be covered by Time of Flight detectors.

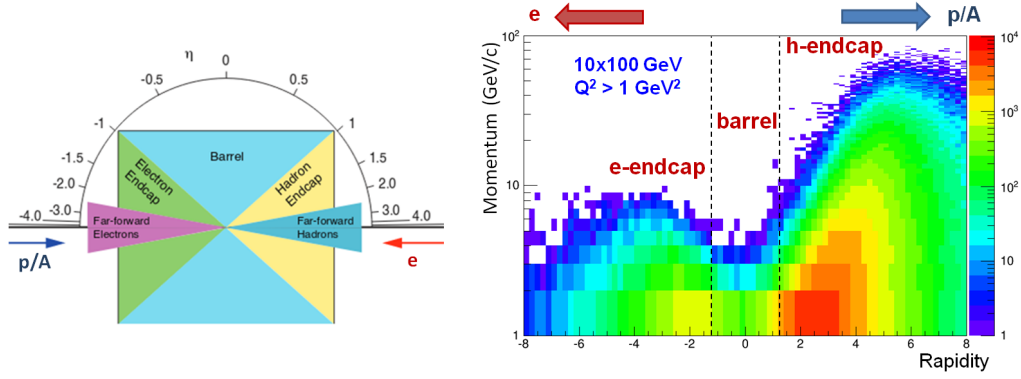


Figure 1. EIC spectrometer concept; left: the generic high level layout with the different main sectors. Right: expected particle phase space for the Semi Inclusive Deep Inelastic Scattering processes.

2 Modular RICH

The mRICH design [6] consists of replica of identical compact RICH modules; each module exploits tiny Fresnel lens to extend the π/K separation from 3 to 10 GeV/c (and e/π up to 2 GeV/c) in the limited space of the EIC electron-endcap (and possibly to other sectors of the spectrometers). The single mRICH module is self-containing (see figure 2 left), with an aerogel radiator, a focusing Fresnel lens and a pixelated photon sensor enclosed in a box of about $14 \times 14 \times 25 \text{ cm}^3$ with internal reflective walls.

The Fresnel lens focuses photons emitted along parallel direction by the aerogel, at relatively large angles, into a single point (see figure 2 right), resulting in a sharper and compact Cherenkov ring and therefore better separation power without the need of a large photon detection area.

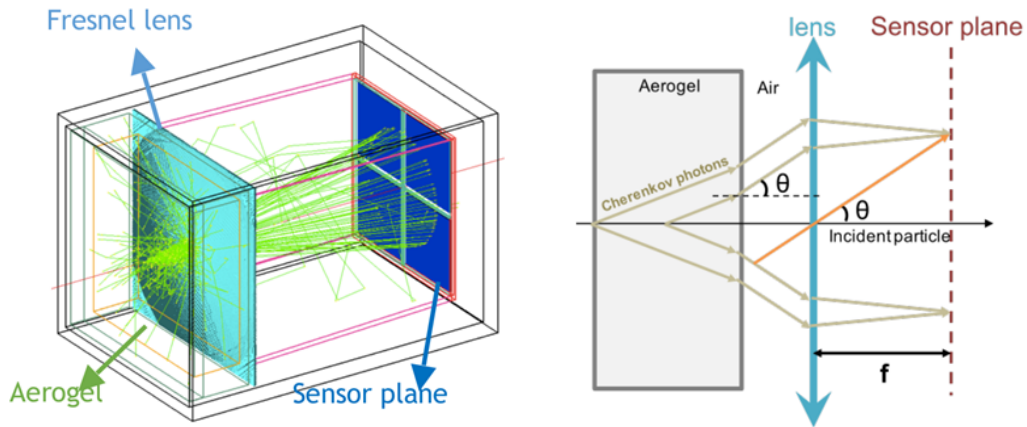


Figure 2. The GEANT4 mRICH model and simulated events (left) and its working principle (right).

The current mRICH key parameters are the 3 cm thick aerogel radiator with $n = 1.03$ refractive index, 6'' (15.24 cm) focal length of the Fresnel lens with $n = 1.47$ and a photo-sensor with $\leq 3 \text{ mm}$ pixel size sitting in the lens focal plane. These specifications are ongoing achievements

of two prototypes and respective tests at Fermilab (both on 120 GeV/c proton beam and 4–8 GeV/c secondary pion beam), extended GEANT4 based simulations and relative analyses. The first prototype beam test in 2016 proved the working principle of the mRICH design. More recently, realistic performances have been measured in the second beam test on the improved prototype; figure 3 reports the measured cumulated rings obtained with two prototype sensor configurations and two different 120 GeV/c proton beam impact points. In fact, both Hamamatsu H13700 Multi Anode PhotoMultiplier Tube (MAPMT) and Silicon PhotoMultiplier (SiPM) photon sensors, with 3 mm pixel size, have been tested; the latter may represent a potential candidate for the final mRICH design, while the former is a consolidated, well known photon sensor useful to understand the detector performances but it cannot be adopted for the final mRICH (as well as the dRICH described below) due to the expected magnetic field in the region where the mRICH shall operate. Both sensors have been readout by the MAROC3 electronics developed for the CLAS12-RICH [7].

The preliminary analysis of the second prototype test, with MAPMT configuration, provided a number of photoelectrons/ring close to 9 (in good agreement with the GEANT4-based Monte Carlo) with a ring photon angular resolution of $\sigma_\theta \approx 6$ mrad which is about twice the Monte Carlo prediction; the discrepancy is likely related to sub-optimal internal alignment and component positioning and a partial characterization of the aerogel tiles; these relevant aspects will be better taken into account in the coming third version of the mRICH prototype, which will further refine the design of the detector.

3 Dual-radiator RICH

The dRICH detector [8] is intended to provide full hadron identification ($\pi/K/p$, better than 3σ apart) from ≈ 3 GeV/c to ≈ 50 GeV/c and, as a byproduct, electron identification (e/π) up to about 15 GeV/c, in the hadron endcap of the EIC detector, covering polar angles of the scattered particles from about 5 up to 25 degree.

The dRICH baseline configuration derived from detailed GEANT4-based simulations, has been consolidated in the first half of 2018; it consists (see figure 4) of 6 identical open sectors (petals) deployed around the beam pipe. Each sector has two radiators: 4 cm thick aerogel with refractive index of $n_{(400\text{ nm})} \approx 1.02$ and 1.6 m C_2F_6 gas with $n_{\text{C}_2\text{F}_6} \approx 1.0008$. The radiators are separated by < 300 nm acrylic filter (to absorb most of the Rayleigh scattered photons coming out from the aerogel); the photons from both radiators share the same outward focusing spherical mirror with 2.9 m radius of curvature and the $4500\text{ cm}^2/\text{sector}$, highly segmented (≈ 3 mm pixel) curved photo-sensors, which sits on the average focal plane, away from the beam and scattered particles acceptance.

The dRICH expected performances have been estimated from simulations which include a 3 Tesla central magnetic field, with aerogel properties and mirror reflectivity from the CLAS12 [7] data. The main contributions to the angular resolutions of both aerogel and gas are reported in the two left plots of figure 5 versus the polar acceptance of the RICH: as expected, the refractive index optical dispersion is the dominant contribution to the aerogel radiator performance while the unknown emission point of the gas photon along the charged particle track competes with the gas chromaticity in the middle of the acceptance; the magnetic field effects on the gas angle reconstruction remain marginal in most of the acceptance.

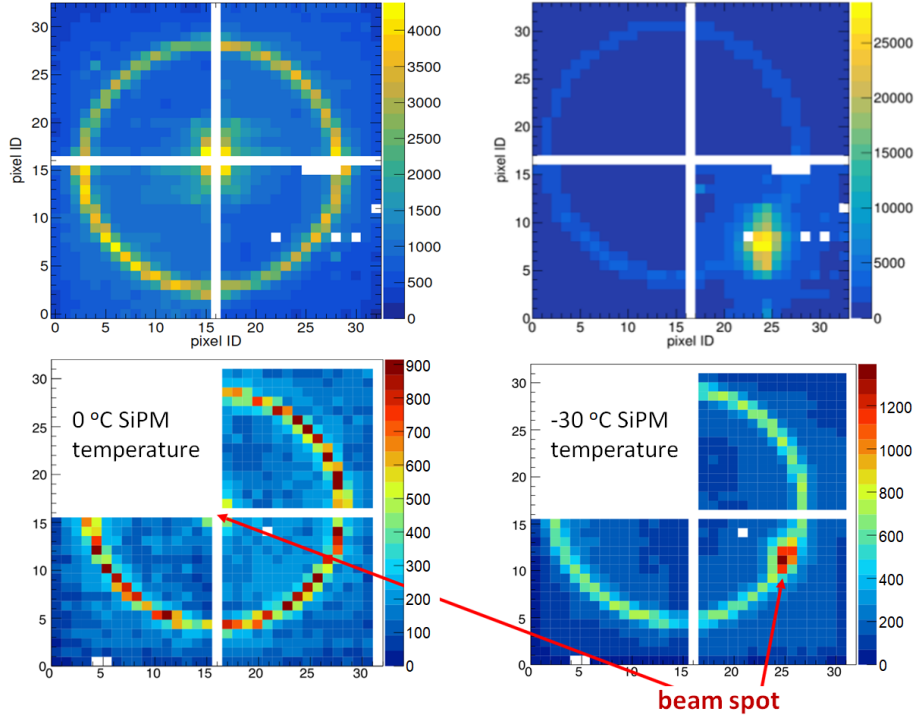


Figure 3. Results of the 120 GeV/c proton beam tests of the mRICH improved prototype, in two different photon sensor configurations: H13700 MAPMT in the upper plots, SiPM in the lower plots (one quadrant is missing because only 3 SiPMs were available for the test). Left and right plots acquired with two different beam impact points, which clearly show one of the main features of the Fresnel lens: its ability to focus photons toward the small sensor surface for quite different impact positions of the impinging charged particles.

Recently, an original approach based on Bayesian optimization has been used to further improve the dRICH baseline performances [9, 10]. The implemented method encodes the detector requirements and then searches for the global maximum of a proper figure of merit keeping the number of iterations required to identify the optimal value relatively small. The figure of merit adopted for the dRICH takes into account the angular separation between pions and kaons in the aerogel-gas transition region (13–15 GeV/c) and at the highest achievable momentum (≈ 60 GeV/c). The right plot of figure 5 shows the obtained improvement in the pion-kaon separation level with respect to the original baseline (legacy performances): a better overlap in the transition region between aerogel and gas and an extended highest momentum are visible. This approach looks promising especially if extended to the simultaneous optimization of several (or whole) spectrometer components.

The above estimated performances and all critical aspects (including technical details that cannot be modeled by Monte Carlo) of the dRICH key components need to be tested and validated by real measurements. For this reason a relatively small scale prototype has been developed and is now going to be implemented. Due to the intrinsic “global” geometry of the dRICH (somehow opposite to the mRICH intrinsic compactness), and in order to minimize costs and size, the prototype is a sort of new detector (see figure 6); it exploits standard vacuum technology to guarantee adequate gas tightness (avoiding expensive and eco-unfriendly gas flowing), two adjustable mirrors to focus aerogel and gas photons into the same photon detector area; the aerogel radiator and photon sensors

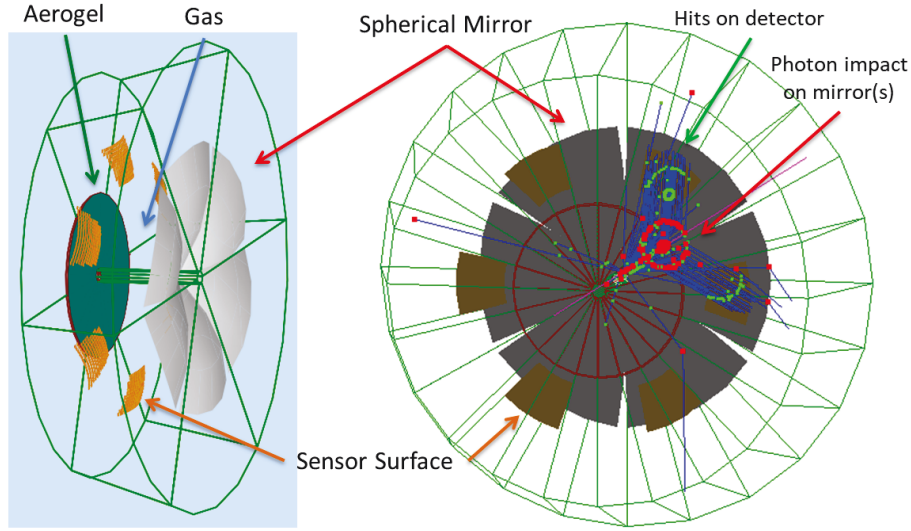


Figure 4. dRICH 3D model: downstream view (left) and upstream view (right) with example of a 10 GeV/c simulated pion: red and green points represent reflection and absorption respectively. In the represented event, the photons reflect on a single mirror and then split on two sectors; the aerogel photons end in two different sensors (two large ring arcs) while the gas photons concentrate in a single sensor (small complete ring); few photons scatter around. The open sectors geometry facilitates the collection of the largest amount of informative photons, keeping relatively small the overall photon detector surface.

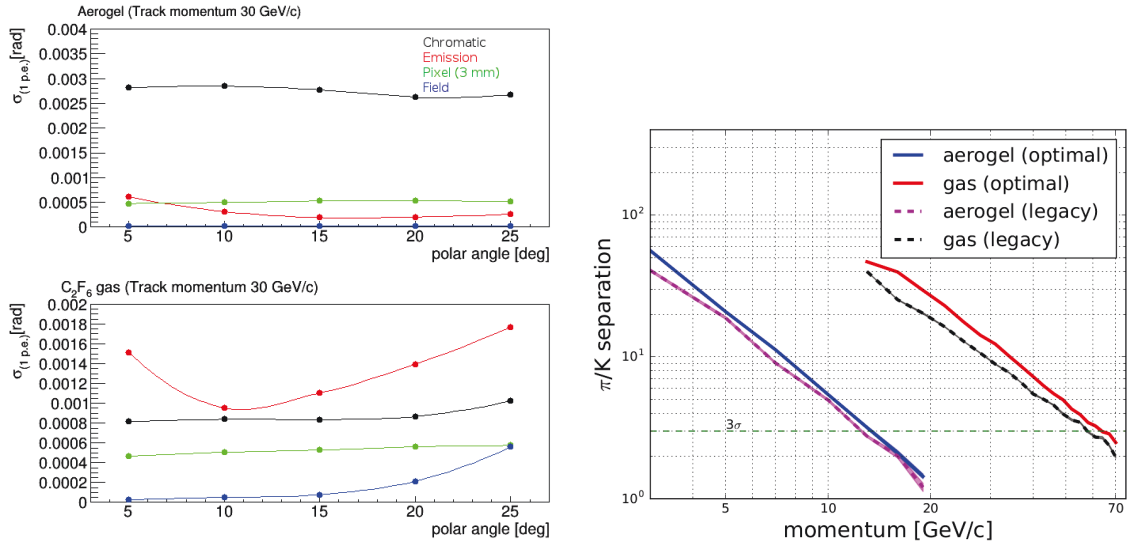


Figure 5. Left: different contributions to the dRICH angular resolution. Right: baseline (legacy) and AI-optimized π/K separation (as number of σ) of the dRICH versus the particle momentum.

are hosted in a protective box isolated from the gas volume by an optically transparent window; front-end electronics will sit on the back of the photon-sensors. The dRICH Monte Carlo simulator, adapted to the prototype geometry for the evaluation of its performances, will eventually be validated by the future prototype tests, and then transferred back to the dRICH full design.

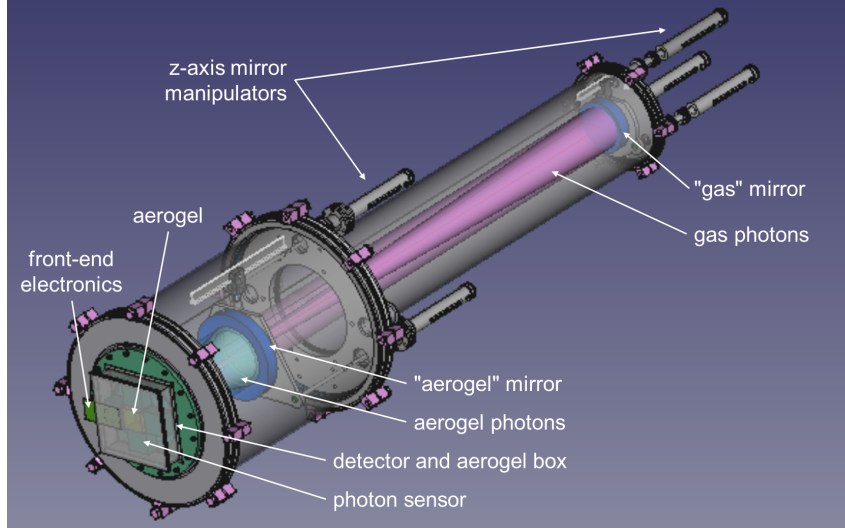


Figure 6. dRICH prototype: the charged particles enter in the bottom left aerogel region, travel along the detector main axis and exit from the top-right window beyond the small “gas” mirror. The relatively large “aerogel” mirror for aerogel photons has a central hole for letting reflected gas photons (pink) reach the sensors. Both mirrors can be aligned by 3 manipulators along the longitudinal axis; they are connected through spherical joints to the mirror supports.

3.1 Event-based reconstruction algorithm

A new event based Cherenkov angle reconstruction method has been introduced in 2018 to evaluate the dRICH performances in realistic physics cases with track multiplicity > 1 , beyond its intrinsic characteristics. The reconstruction uses the track-based Inverse Ray Tracing (IRT) method, adopted in the HERMES dual radiator RICH [11], to determine the emission angle corresponding to each photon hit, given a hypothesis on the particles associated to each track in the event: the likely correct hypothesis is the one that maximizes an appropriate likelihood. However, in order to reduce the computational effort (number of hypotheses),² the method (see flow chart in figure 7) splits the reconstruction into two main steps (and corresponding likelihood functions): given a particle hypothesis, each hit (detected photon) is sequentially associated to tracks/radiators using a first likelihood $L1$; once all hits are associated, one estimates a global likelihood ($L2$) for each track-particle combination and then it chooses the combination yielding the maximum $L2$. The likelihood functions account for the angular correlation (through Gaussian-derived distribution) and the number of detected photons (described by a Poissonian distribution). The reconstruction performances have been evaluated on deep inelastic PYTHIA [12] generated physics events: about 40% of them have multiple tracks and 50% of those have overlapping rings; the results (see figure 8) confirm the extended momentum coverage with no noticeable degradation introduced by the reconstruction itself. A detailed analysis of the two likelihood functions is underway to maximize their effectiveness in prioritizing the correct hypothesis.

²As an example, given $N_p = 4$ potential particle types (electron, pion, kaon and proton) for a typical event with $N_t = 2$ tracks (crossing the $N_r = 2$ radiators), $N_h = 15$ detected hits, the total number of combinations of potential particle hypotheses, tracks, radiators and hits are $N_p^{N_t} \cdot (N_t \cdot N_r + 1)^{N_h} \approx 488$ billion (including a virtual track for the noise); the proposed reconstruction method reduces this number to $N_p^{N_t} \cdot (N_r \cdot N_t + 1) \cdot N_h = 1200$.

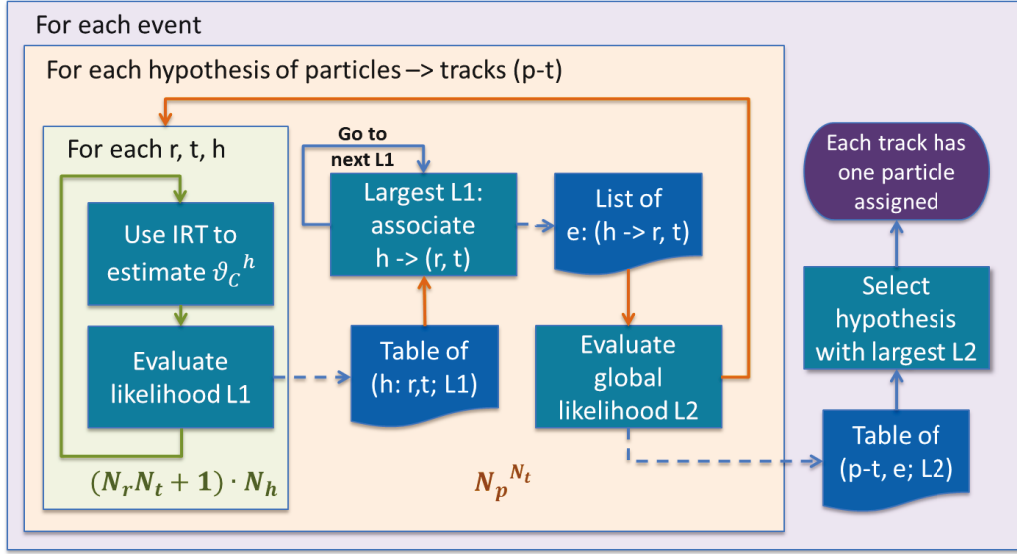


Figure 7. The schematic flow chart of the event based reconstruction algorithm; the 3 largest boxes represent nested loops; the first step in the inner loop is the estimate of Cherenkov angle θ_C^h . e, h, p, r and t are the event, hit, particle type, radiator and track indices respectively; $L1$ and $L2$ are the two likelihood functions described in the text. N_p, N_r, N_t and N_h are the number of potential particle types, radiators, tracks and hypotheses.

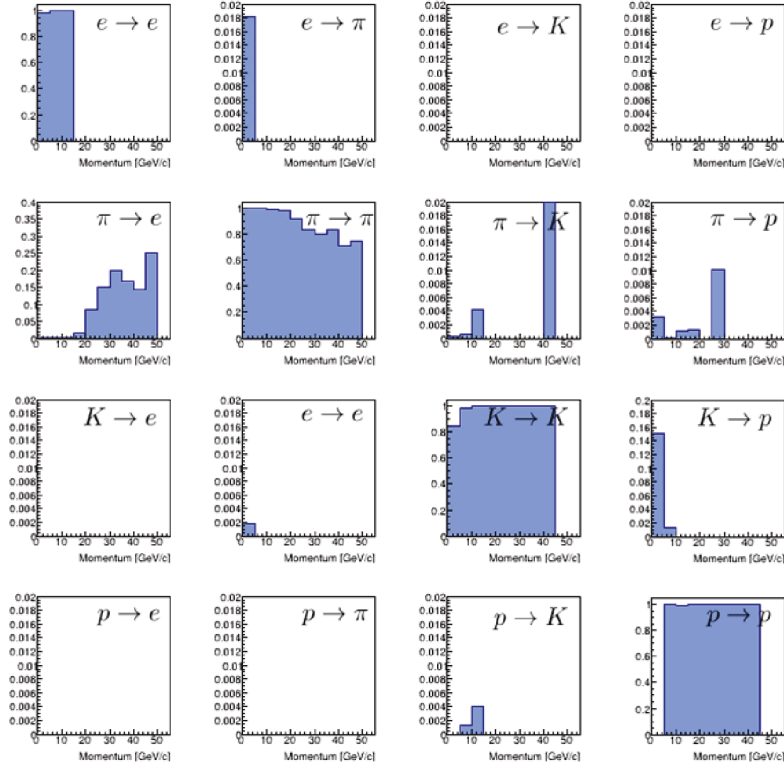


Figure 8. dRICH identification performances by the event-based reconstruction method applied to deep inelastic PYTHIA physics.

4 Conclusions

The above-presented RICHes have to follow different development paths due to the rather opposite geometries and optics: the compactness and lens-based optics of the mRICH allowed an almost immediate and relatively inexpensive prototyping while the large, difficult to scale down, dRICH needed a longer definition phase before moving to first prototyping. The mRICH is now going to test its third prototype while the dRICH has entered into the implementation of the prototype.

On the other hand, both RICHes are currently sharing photo-sensors and readout electronics developments (going on within the EIC-eRD14 and other EIC related consortia) which represent important components in both detectors, subjected, to different extents, to magnetic field and radiation damage relevant restrictions.

Acknowledgments

Part of the previous work is based upon work supported by the U.S. Department of Energy, Office of Science, Office of Nuclear Physics under the EIC R&D funding scheme.

References

- [1] A. Accardi et al., *Electron Ion Collider: The Next QCD Frontier*, *Eur. Phys. J. A* **52** (2016) 268 [[arXiv:1212.1701](#)]-
- [2] E.C. Aschenauer et al., *eRHIC Design Study: An Electron-Ion Collider at BNL*, [arXiv:1409.1633](#).
- [3] S. Abeyaratne et al., *MEIC Design Summary*, [arXiv:1504.07961](#).
- [4] E.C. Aschenauer et al., *Electron Ion collider: Detector Requirements and R&D Handbook*, <http://www.eicug.org/web/content/detector-rd> (2020)
- [5] X. He, *RICH detector development for the electron-ion collider experiments*, *Nucl. Instrum. Meth. A* **952** (2020) 162051.
- [6] C.P. Wong et al., *Modular focusing ring imaging Cherenkov detector for electron-ion collider experiments*, *Nucl. Instrum. Meth. A* **871** (2017) 13.
- [7] M. Contalbrigo, *Single photon imaging with the CLAS12 RICH detector*, in proceedings of *International Workshop on Fast Cherenkov Detectors, Photon detection, DIRC design and DAQ*, Giessen, Germany, 11–13 September 2019.
- [8] A. Del Dotto et al., *Design and R&D; of RICH detectors for EIC experiments*, *Nucl. Instrum. Meth. A* **876** (2017) 237.
- [9] E. Cisbani et al., *AI-optimized detector design for the future Electron-Ion Collider: the dual-radiator RICH case*, [arXiv:1911.05797](#).
- [10] C. Fanelli, *Machine learning for RICH counters*, in proceedings of *International Workshop on Fast Cherenkov Detectors, Photon detection, DIRC design and DAQ*, Giessen, Germany, 11–13 September 2019.
- [11] N. Akopov et al., *The HERMES dual-radiator ring imaging Cherenkov detector*, *Nucl. Instrum. Meth. A* **479** (2002) 511 [[physics/0104033](#)].
- [12] PYTHIA Home Page, <http://home.thep.lu.se/Pythia/> (2020)